

Pull-out behaviour of straight and hooked-end steel fibres under elevated temperatures

Sadoon Abdallah, Mizi Fan,* and K.A. Cashell

*College of Engineering, Design and Physical Sciences, Brunel University
Uxbridge, UB8 3PH, London, United Kingdom*

Abstract

This paper presents the results of an experimental investigation into the effect of elevated temperature on the steel fibre-matrix bond characteristics. A series of pull-out tests on straight and hooked-end fibres embedded in four different cementitious matrixes, namely normal strength concrete (NSC), medium strength concrete (MSC), high strength concrete (HSC) and ultra-high performance mortar (UHPM) were performed. Ninety days after casting, the specimens were heated to target temperatures of 100, 200, 300, 400, 500, 600, 700 and 800°C, respectively. The initial and residual thermal and mechanical properties of the concrete were investigated. It was shown that while the variation in compressive strength and pull-out response for different temperatures is relatively small up to 400°C, further increase in temperature results in a reduction in the pull-out strength, especially for the temperature greater than 600°C. At 800°C, the maximum pull-out load of the hooked-end fibres with NSC, MSC and HSC decreased by 54%, 64% and 56%, respectively.

Key words:

Pull-out behaviour; Bond mechanisms; Elevated temperatures; Hooked-end fibres; Straight fibres

**Corresponding author: Professor Mizi Fan, Head of Civil Engineering Department and Research Director, Brunel University, Email: mizi.fan@brunel.ac.uk, Tel.: +44 189 5266466*

1. Introduction

Fire remains one of the major hazards for high-rise buildings, tunnels and other infrastructure. For this reason, many researchers have spent considerable effort towards understanding the effects that elevated temperatures have on building materials and elements [1]. This is particularly true in more recent times for newer materials, such as steel fibre reinforced concrete (SFRC). SFRC is now widely used as a primary construction material in a variety of applications due to its excellent performance in improving the tensile response of concrete and also its ability to control crack propagation [2,2,3,3,4]. However, like most other construction materials, the exposure of SFRC to high temperature results in a significant deterioration of the physical and mechanical properties of both component materials and their inter-relationship (i.e. bond) [5]. Bond is the mechanism through which tensile forces are transmitted between the steel fibres and the surrounding cement paste. A part of these forces are resisted by the cement paste, whilst the remainder is resisted by the fibres. The interfacial bond properties between the fibres and cement paste play a crucial role in controlling the mechanical properties of SFRC at both room and elevated temperatures. Therefore, the knowledge of the bond relationship is the first key step towards understanding the behaviour of SFRC structural elements at an elevated temperature. The bond characteristics are commonly assessed using the single fibre pull-out test, which is able to determine the interfacial properties between the fibres and the surrounding cementitious matrix [6].

The mechanical properties of SFRC at room temperature have received considerably more attention from the research community compared to those at the elevated temperature [7]. More recent attempts on the SFRC under the elevated temperature mainly focus on the mechanical rather than the thermal properties [8-10]. The primary mechanical properties that influence the fire performance of SFRC members are the compressive strength, tensile strength, elastic modulus and the stress-strain response in compression. Although steel fibres may not offer any obvious advantage from a fire-endurance point of view, it has been shown that steel fibres can be considered as an effective way in delaying the spread of cracking, and hence potentially improve the performance of concrete after exposure to high temperature [11]. However, due to variations in concrete strength, test methods and heating conditions, there is a lack of consensus on the SFRC behaviour under an elevated temperature in the available literatures.

The degradation of the mechanical properties of concrete at high temperature is mainly due to the physicochemical bond changes that occur in the cement paste and aggregate as well as

thermal incompatibility between the cement paste and the aggregate [12]. The temperature-dependent properties also vary with the concrete strength. For example, researchers have found that high strength concrete (HSC) is more likely to experience dramatic spalling failure at a given elevated temperature compared with normal strength concrete (NSC), mainly owing to the finer pore structure in HSC [13]. It has also been shown that the occurrence of explosive spalling is more likely in HSC than NSC at similar levels of elevated temperature [14]. There are a number of measures which can be taken to effectively alleviate spalling under high temperatures for HSC such as the addition of polypropylene fibres [15], steel fibres [16] or hybrid fibres (steel and polypropylene fibres) [7], as well as protecting the exposed concrete surface with a thermal barrier [12].

As stated before, it is essential to have a proper understanding of the bond relationship between the steel fibres and the concrete matrix at elevated temperature in order to evaluate the deterioration in mechanical properties of SFRC; nevertheless, little information on this topic is available in the literature. In this context, the current paper presents an experimental study into the pull-out behaviour of both straight and hooked-end steel fibres under a range of elevated temperatures. The main objective is to investigate the bond mechanisms associated with the pull-out behaviour, and how these are affected by elevated temperatures. Four groups of cementitious mixtures with an initial compressive strength ranging between 33 and 148 MPa are included in the study. The results are essential in order to develop a better understanding of the effect of high temperature on the bond-slip characteristics and to further assess the degree of deterioration in mechanical properties of SFRC after high temperature exposure. The results of the experiments are presented and discussed in detail, with particular attention given to the most salient parameters such as concrete strength and fibre type.

2. Experimental program

2.1. Materials and sample preparation

Table 1 presents the four grades of concrete which were included in the experimental programme, namely normal strength concrete (NSC), medium strength concrete (MSC), high strength concrete (HSC) and ultra-high performance mortar (UHPM). The NSC mix design was prepared using ordinary Portland cement whilst the other three mixes all employed high strength Portland cement (i.e. CEM II 32.5R and CEM III 52.5N, respectively, in accordance with European standard EN 197-1 [17]). Silica fume, ground quartz and fly ash were also

used for the preparation of the MSC, HSC and UHPM mixtures. Around 60 % of the crushed granite aggregates were 6 mm in size and the remaining 40 % were 10 mm. Two types of sand were used in experimental programme. As presented in Table 1, coarse grain sand (C.G.S., 0-4 mm) was used in the NSC, MSC and HSC mix design and very fine grain sand (F.G.S., 150-600 μ m) was used in the UHPM concrete. A superplasticizer called TamCem23SSR was used to enhance the workability of the HSC and UHPM mixtures.

The geometrical properties of hooked-end fibres are depicted in Fig. 1a. The steel fibres used in this study were the commercially-available Dramix hooked-end fibres (3D 65/60 BG fibres) which were 60 mm in length (l_f), 0.90 mm in diameter (d_f) and had an aspect ratio of 65 and a yield tensile strength (f_y) of 1150 N/mm². The measured values of the hook geometry, namely l_1 , l_2 , α and β (as shown in Fig. 1) are given in Table 2. For the tests using straight fibres, the same samples were used with the hooked-ends cut off, as illustrated in Fig. 1b.

The pull-out tests on single steel fibres were performed using cubes with a side dimension of 100 mm for NSC, MSC and HSC, and cylinders with a diameter of 100 mm and height of 50 mm for the UHPM samples (this is because of the finer aggregates). In each test specimen, a single steel fibre was carefully placed through a hole which was made in the bottom of moulds. The embedded length (l_E) was one half of the overall fibre length (i.e. 30 mm). For each concrete mix, three additional cubes (again 100mm in size) were prepared in order to determine the compressive strength of the mixture. The concrete was prepared using a laboratory pan mixer for the NSC, MSC and HSC, and a hobart mixer for UHPM (which is only used for fine materials without coarse aggregates). During preparation, the dry components were firstly mixed for approximately 1 minute before water and the superplasticizer (for the HSC and UHPM) were added. This was then mixed for 11 minutes, which experience has shown is appropriate to result in a homogenous mixture. After casting and vibration, the specimens were covered with a thin polyethylene film to avoid retain the escaping moisture and left for 24 hours at room temperature. The specimens were then removed from moulds and cured for a further 28 days in the conditioning chamber, where the temperature was held at 20 \pm 2 $^{\circ}$ C and the relative humidity 96 \pm 4 %. All specimens were tested at an age of 90 \pm 2 days and the average value of three specimens was adopted, both for the compressive strength and pull-out tests.

2.2. Heating scheme

After 90 days, the pull-out and compressive strength specimens were directly placed in the electric furnace. The free end of the steel fibre for the pull-out specimens was covered with heat insulation before placed in the furnace. A controlled furnace was used which is capable of achieving a maximum temperature of 1100°C and a maximum heating rate of 36°C/min. In this study, the specimens were heated to a maximum temperature of either 100, 200, 300, 400, 500, 600, 700 or 800°C at a constant rate of 20°C/min, based on the recommendations of Haddad and Shinnas [18]. Once the target temperature was reached, it was held constant for one hour and then the specimens were allowed to cool in the furnace for 1 day before the compressive strength and pull-out tests were conducted. The temperature-time curve is presented in Fig. 2.

2.3. Test setup

The pull-out tests were performed on the cooled specimens using a specially designed grip system, as illustrated in Fig. 3, which was attached to an Instron 5584 universal testing machine. The grips were designed such that the forces applied to the fibre provided a true reflection of the real situation experienced by fibres bridging a crack. The body of the gripping system was machined in a lathe using mild steel and had a tapered end to allow the insertion of four M4 grub screws (Fig. 3). These were then tightened around the steel fibre to an equal torque for an even distribution of gripping pressure to minimise the deformation of the fibre ends and avoid breakage at the tip. Two linear variable differential transformer (LVDT) transducers were used to measure the distance travelled by the steel fibre relative to the concrete face during testing (i.e. the pull-out distance). They were held in place using aluminium sleeves on either side of the main grip body (Fig. 3). The LVDT's had ball bearings at the tips to allow for accurate readings on the face of the samples. The sample was secured to the Instron base using clamps with riser blocks and M16 studs. The specimen was positioned on a brass round disc to remove any discrepancies in the sample base and allow for distortion. In all pull-out tests, a displacement rate of 10 µm/s was adopted.

3. Results and discussion

3.1. Mechanical and thermal properties of cementitious mixes at elevated temperatures

3.1.1. Compressive strength

The results from the compressive strength tests on all concrete mixes (NSC, MSC, HSC and UHPM), following exposure to elevated temperatures, are summarized in Table 3. It is noteworthy that the UHPM results are only presented up to 400°C (Table 3) because above these temperatures, the specimens exploded in the furnace; this is discussed later in more detail. While the compressive strength does not vary significantly within the temperature range from 20 to 400°C for all the mixes tested. The strength of NSC, MSC and HSC, reduces slightly at 100°C and then regains almost to its full ambient strength at 200°C. The decrease in strength at 100°C temperature may be attributed to initial moisture loss, while the regain of strength at 200°C temperature is likely to be due to an acceleration in the pozzolanic reaction and moisture migration in the concrete [8,19].

The compressive strength at elevated temperature (f_{ct}) normalised to the corresponding ambient temperature value (f_c) with changing temperature was given in Fig. 4. It is clear that up to around 400°C, there are insignificant changes in the compressive strength with temperature. This is in agreement with other results reported previously [20]. Above 400°C, there is gradual degradation of strength with increasing temperature. For the NSC, MSC and HSC, the loss of compressive strength at 600°C in these tests was around 45%, 35% and 52%, respectively (Fig. 4). This significant loss in compressive strength may mainly be attributed to the loss of chemically-bound water due to dehydration and disintegration of hydrated calcium silicate (C-S-H) gel in the concrete. Once the target temperature reaches 800°C, the compressive strength of NSC, MSC and HSC was only 33%, 42% and 47% of its original strength at ambient temperature, respectively. Therefore, it can be deduced that high temperatures in the range of 600-800°C are critical in terms of strength loss.

The behaviour of the NSC, MSC and HSC mixes differed significantly from that of UHPM in the tests above 400°C, particularly in terms of the failure mode. Above 400°C, the UHPM specimens experienced severe explosive spalling as opposed to the other specimens which failed by spalling of small fragments from the specimen top surface (Fig. 5). This phenomenon is attributed to the lower permeability of UHPM compared with the other mixes

which limits the ability of water vapour to escape from the pores. For this reason, the results of UHPM are only presented up to 400°C to allow fair comparison with the other mixes.

3.1.2. Mass loss

The mass of each specimen was measured before and after heating in order to determine the mass loss as a result of exposure to elevated temperature (Table 3), which is presented as the percentage mass loss relative to the corresponding value at ambient temperature (M_{loss}). It is apparent that the exposure to high temperatures results in an increasing loss of mass. It is interesting that the mass loss is minimal (i.e. <3 %) up to around 300°C, but above 300°C, the NSC and MSC mixes behave very similarly and experience higher mass loss than the HSC (the UHPM is not included above 400°C due to the previously discussed spalling failure mechanism). The greater mass loss in these materials may be attributed mainly to their more permeable microstructure compared to HSC. At 800°C, the loss in mass in the NSC, MSC and HSC specimens is 11%, 10% and 8%, respectively. The trend of mass loss was very similar to that the compressive strength change, showing a close correlation between compressive strength and mass loss. The results also indicate that there may be a certain loss of free water, bound water and also chemical water at high temperature exposure. The loss of water, especially bound water and chemical water, not only changes the integrity of internal structure of concrete, but also the transportation of vapour could affect the compact of concrete.

3.2. Pull-out behaviour at elevated temperature

3.2.1. Straight fibres

3.2.1.1. Pull-out load-slip response

In order to determine the interfacial bond characteristics between the simplest form of fibre (i.e. straight fibres) and the surrounding concrete, the end portions of the hooked-end fibres were removed, as shown in Fig. 1b. For straight fibres, the bond between the fibre and the concrete is generated only by friction and the chemical adhesion between the two materials and there is no significant mechanical interlocking or anchorage. The load-slip behaviour measured during the tests for the NSC, MSC, HSC and UHPM samples at the full range of tested temperatures are presented in Fig. 6. The maximum pull-out load ($P_{peak,s}$), the corresponding slip at $P_{peak,s}$ ($S_{peak,s}$) and the total amount of work done in the pull-out ($W_{total,s}$), which is calculated as the area under the pull out load-slip curve at each temperature, are given in Table 3. It can be seen that the pull-out behaviour of the straight

fibres is mainly characterized by a rapid increase followed by a sudden drop in pull-out load, indicating that the fibre debonds significantly from the concrete in a rapid manner. Afterwards, the pull-out load continues to decrease with an increase in slip. As stated before, for the straight fibres, bond is made up only of chemical adhesion and friction with no mechanical interlock. So, once these mechanisms are overcome, the fibre pulls under low pull-out resistance.

3.2.1.2. Effect of matrix strength on pull-out behaviour of straight fibres

With reference to the $P_{\text{peak,s}}$ and $W_{\text{total,s}}$ values at ambient temperature (Table 3), it is observed that, as expected, as the compressive strength of the matrix increases (i.e. from NSC to MSC to HSC to UHPM), both the maximum pull-out load and the pull-out work done also increase. After exposure to elevated temperature, there is a decrease in both $P_{\text{peak,s}}$ and $W_{\text{total,s}}$ with increasing temperature for all concrete types. This is because of the gradual degradation in bond strength that occurs at elevated temperature owing to both physical and chemical transformation of concrete. These interactions progressively weaken and crack the concrete, resulting in local breakdowns in the bond between the cement paste and the fibres.

The pull-out behaviour of the straight fibres embedded in all three concrete mixes followed a similar trend at high temperatures. Following heating of the NSC, MSC, HSC and UHPM to 400°C, their peak pull-out load decreased by 55%, 40%, 21% and 51%, respectively, relative to the corresponding ambient temperature values (Table 3). This rapid degradation of $P_{\text{peak,s}}$ can be attributed to the significant loss of chemically-bound water at this temperature which causes dehydration and the disintegration of the C-S-H bond in the concrete. For the UHPM mixture, $P_{\text{peak,s}}$ reduces significantly compared with the other mixtures in the range of 20-400°C temperature. This may be attributed to the fact that UHPM is produced with a relatively low water/binder (W/B) ratio as well as a relatively high binder content, which combine to form a denser microstructure with lower permeability, compared to the other concrete mixes. This can induce internal cracking between the cement paste and the aggregate due to the evaporation of free water and expansion of the paste; thus, the fibre-matrix interfacial bond strength is reduced significantly.

On the other hand, at higher temperatures in the range between 600-800°C, NSC, MSC and HSC exhibit significantly lower values of $P_{\text{peak,s}}$, relative to their corresponding ambient values. The loss in pull-out strength of HSC is more abrupt in comparison to the gradual loss

which occurred for the NSC and MSC in the 500-800°C temperature range. This sharp reduction in bond strength for HSC specimens may be due to its relatively low water/binder ratio which results in the dehydration of the cement paste by reducing the free water in the concrete. At 800°C, the $P_{\text{peak,s}}$ of the NSC, MSC and HSC mixes dropped by around 84%, 64% and 79%, respectively, from their corresponding ambient values. Since the pull-out resistance of straight fibres is primarily controlled by the physicochemical adhesion properties between the fibre and matrix [21], the sharp reduction in $P_{\text{peak,s}}$ can be attributed to the significant changes in the physicochemical bond properties between the fibre and matrix at this temperature. Accordingly, it is deduced that the microcracks may be developed in the concrete at this temperature in the region around the fibre which causes the resistance to pull-out to diminish significantly. Also, from Table 3 it is interesting to observe that although the NSC produced with the highest W/B ratio, it exhibits the greatest reduction in bond strength at 800°C. According to Arioz [1] the decrease in W/B ratio to 0.4 has no significant effect on concrete strength losses and higher loss was observed for mixtures with higher W/B ratios. In addition, the absence of admixtures in the NSC mix may also contribute to a poor interfacial bond strength between the cement paste and aggregate or reinforcing fibre.

3.2.2. Hooked-end fibres

3.2.2.1. Pull-out load-slip response

The pull-out load-slip curves for the specimens with hooked-end fibres embedded in concrete are very different from these of straight fibres (Fig. 7). It is apparent that the level of bond strength is significantly higher for the hooked-end fibres. The different mechanisms of bond may have developed in the hooked-end fibres. The straight fibres rely entirely on friction and adhesion to generate bond, whereas, in addition to these mechanisms, the hooked-end fibres also develop mechanical interlock to resist slippage. The $P_{\text{peak,h}}$ is 49%, 57%, 55%, and 47% higher than that of $P_{\text{peak,s}}$ pulled from the NSC, MSC, HSC and UHPM, respectively. The most significant difference is that after the peak pull-out load has been achieved, the bond strength diminishes gradually and then experiences a second gain in strength at around 4-5 mm of slip; this is the activation of the mechanical interlock which develops once adhesion has been overcome and some slip has occurred. The loss of pull-out load post- $P_{\text{peak,h}}$ is more gradual in the hooked-end fibres compared with the straight fibres owing to the more complex bond mechanisms involved.

From the test results (Fig. 7 and Table 3), it is clear that the elevated temperature pull-out load-slip relationship can be separated into two temperature ranges, namely 20-400°C and 400-800°C. Between 20°C and 400°C, the pull-out behaviour of the hooked-end fibres is not significantly influenced by the change in temperature. For the NSC mix, the pull-out force decreases at 100°C compared with the corresponding ambient value and then actually increase to a value greater than occurred at ambient temperature at 200°C and 300°C (Table 3). For the MSC and UHPM concrete, $P_{\text{peak,h}}$ is higher at each temperature interval up to 300°C compared with the corresponding ambient value (Table 3). On the other hand, for the fibres embedded in HSC, the bond strength begins to diminish once the sample has been exposed to any amount of elevated temperature. Regarding the increase in bond strength that occurs in some samples in the 100-300°C temperature range, this is attributed to rehydration in the concrete mix, acceleration in the pozzolanic reaction, in addition to moisture migration; these phenomena combine to result in an improvement in the bond strength. It is noteworthy that this was not observed in the tests using straight fibres and therefore, it can be deduced that only the mechanical interlocking bond mechanism is affected by these chemical changes in this temperature range. After exposure to 400°C, the hooked-end fibres in NSC, MSC and HSC all demonstrate a decrease in pull-out load, compared with their equivalent ambient values. The UHPM bond strength also decreases compared to the values in the 100-300°C range, but is still slightly higher than the force achieved at ambient temperature.

In the higher temperature range between 400°C and 800°C, there is a more significant loss in the pull-out strength with increasing temperature, especially above 600°C, as the bond strength between the fibre and the concrete diminishes. In this temperature range, there is a significant loss of moisture as well as a degradation of the concrete microstructure which leads to the development and propagation of micro- and macro-cracks at the fibre-concrete interface. As a result, the fibres are completely pulled out without full deformation or straightening of the hooks. This phenomenon explains the difference in shape of the curves for NSC, MSC and HSC exposed to 700°C and 800°C compared with those in the 20-600°C temperature range.

3.2.2.2. Effect of matrix strength on pull-out behaviour of hooked-end fibres

It can be seen that the maximum pull-out load ($P_{\text{peak,h}}$) and total work during pull-out ($W_{\text{total,h}}$) of the hooked-end fibres at room temperature increases as the matrix compressive strength increases (Fig. 7 and Table 3), as expected. At room temperature, the highest levels of bond

strength are found in the HSC and UHPM samples, leading to significantly higher values for $P_{\text{peak,h}}$ and $W_{\text{total,h}}$ compared with the other mixes. However, at elevated temperatures, the various concrete mixes demonstrate some different behaviour patterns. The NSC and MSC matrixes tend to have more modest peak pull-out loads but then lose their bond strength in a more gradual manner compared with the HSC and UHPM mixes. For the UHPM concrete, some of the fibres partially ruptured at the hook end during the pull-out process, as shown in Fig. 8, causing a sudden reduction in pull-out load. Although these fibres ruptured at slips of between 2 and 4.5 mm, the remaining part of the fibre continued to transmit the pull-out loads (Fig. 7d). For NSC and MSC, the influence of concrete compressive strength on the maximum pull-out load becomes less important when the temperature exceeds 500°C. It can be seen that these two concretes have quite similar values throughout the (600-800°C) temperature range.

As expected, when the highest temperature of 800°C was applied to the specimens, the lowest value of P_{peak} was recorded. The NSC, MSC and HSC specimens lost 54%, 63% and 56%, respectively, of their corresponding ambient temperature maximum pull-out loads at 800°C. These values are all within +/-5% of each other, showing that the variation in the loss of pull-out load between the different concretes is not very significant. Nevertheless, HSC has superior bond strength compared with the other concretes and therefore displays better pull-out response even at higher temperatures. It is noteworthy that the load-slip curves in Fig 8a-c show a difference in behaviour of $P_{\text{peak,h}}$ at 700-800°C compared with lower temperatures. From 20-600°C, as stated before, the pull-out load reaches a peak value of $P_{\text{peak,h}}$ at around 1-2 mm of slip, and this is followed by a gradual reduction in the load, followed by a gentle increase at around 4 mm of slip (due to the activation of mechanical interlock). Thereafter, the pull-out load decreases progressively until it reaches a residual value at around 5-6 mm of slip. On the other hand, for the samples exposed to 700-800°C, this double peak phenomenon is not observed. This is most likely because the chemical adhesion and friction is lost due to the exposure to these high temperatures and significant bond is developed only from mechanical interlock. This is verified in the results from the tests on straight fibres (Fig. 6) which show very low values of pull-out load for specimens heated to 700-800°C. More detailed analysis of the influence of elevated temperatures on the pull-out response is being seen in next section.

3.2.2.3. Evaluation of the deformation and straightening of the hook

In order to further understand the influence of elevated temperature on the pull-out response of hooked-end fibres, the deformation and straightening behaviour of fibres pulled out from different concrete matrixes have been examined using optical microscopy (OM). The OM images of the hooked-end fibres pulled-out from NSC, MSC, HSC and UHPM after heating to 20, 400, 600 and 800°C are presented in Fig. 9. These images show that the hooked-end fibres embedded in all matrixes at 20 and 400°C are almost completely deformed and straightened during pull-out; this occurs to a greater extent in HSC and UHPM compared with NSC and MSC. However, at temperatures of 600°C and above, it can be seen that the fibre hook embedded in the NSC, MSC and HSC matrixes did not straighten to the same extent. The lower level of deformation and straightening of the hook at higher temperatures may be attributed to the significant degradation of the matrix and local crushing at the fibre-concrete interface. Another possible reason for this may also be related to the surface damage of the fibres caused by oxidation, which results in deterioration of the bond between fibre and matrix. This also provides an explanation for the similar values of $P_{\text{peak,h}}$ for hooked-end fibres embedded in NSC and MSC throughout the 600-800°C temperature range.

4. Conclusions

The effect of elevated temperatures on the bond characteristics between steel fibres and the surrounding concrete was investigated through an extensive experimental programme. From the results of this investigation, the following conclusions can be made:

- 1) The NSC, MSC and HSC specimens retained 88%, 93% and 90% of their compressive strength after exposure to 400°C, and this was further reduced to 46%, 37% and 45% after exposure to 800°C, respectively. The temperature deduced degradation was related to the mass loss, which though at 800°C, the mass losses of NSC, MSC and HSC specimens were only 11 %, 10 %, and 8 % of their original values, respectively.
- 2) The pull-out strength of straight fibres was shown in the experiments to gradually decrease with increasing temperature. At 800°C, the peak pull-out load reduced to 16%, 36% and 21% of the corresponding ambient values, for NSC, MSC and HSC, respectively.
- 3) The influence of high temperature on the pull-out response of hooked-end fibre was twofold. In the range of 20-400°C, the pull-out behaviour of hooked-end fibres did not vary

significantly with temperature. However, above 400°C, the pull-out response of hooked-end fibres embedded in all three concrete matrixes gradually decreased with temperature. At 800°C, the peak pull-out load reduced to 46%, 37% and 44% of the corresponding ambient values, for NSC, MSC and HSC, respectively.

4) The reduction in pull-out strength for all mixtures correlated very well with the corresponding decrease in compressive strength. However, the compressive strength of matrix does not have a significant effect on the peak pull-out load of the hooked-end fibres embedded in NSC and MSC in the 600-800°C temperature range.

5) It was shown that exposure to higher temperatures (between 600 and 800°C) had a significant influence on the deformation and straightening of the hook of steel fibres.

Acknowledgments

The first author gratefully acknowledges the financial support of the Ministry of Higher Education and Scientific Research of Iraqi Government for this Ph.D. project.

References

- [1] O. Arioz, Effects of elevated temperatures on properties of concrete, *Fire Saf. J.* 42 (2007) 516-522.
- [2] F. Laranjeira, C. Molins, A. Aguado, Predicting the pullout response of inclined hooked steel fibers, *Cem. Concr. Res.* 40 (2010) 1471-1487.
- [3] E. Zile, O. Zile, Effect of the fiber geometry on the pullout response of mechanically deformed steel fibers, *Cem. Concr. Res.* 44 (2013) 18-24.
- [4] S. Abdallah, M. Fan, X. Zhou, S. Geyt, Anchorage Effects of Various Steel Fibre Architectures for Concrete Reinforcement, *International Journal of Concrete Structures and Materials.* (2016) 1-11.
- [5] T. Pothisiri, P. Panedpojaman, Modeling of bonding between steel rebar and concrete at elevated temperatures, *Constr. Build. Mater.* 27 (2012) 130-140.
- [6] S. Abdallah, M. Fan, D.W.A. Rees, Analysis and modelling of mechanical anchorage of 4D/5D hooked end steel fibres, *Mater Des.* 112 (2016) 539-552.

- [7] P. Pliya, A. Beaucour, A. Noumowé., Contribution of cocktail of polypropylene and steel fibres in improving the behaviour of high strength concrete subjected to high temperature, *Constr. Build. Mater.* 25 (2011) 1926-1934.
- [8] W. Khaliq, V. Kodur, Thermal and mechanical properties of fiber reinforced high performance self-consolidating concrete at elevated temperatures, *Cem. Concr. Res.* 41 (2011) 1112-1122.
- [9] C.S. Poon, Z.H. Shui, L. Lam, Compressive behavior of fiber reinforced high-performance concrete subjected to elevated temperatures, *Cem. Concr. Res.* 34 (2004) 2215-2222.
- [10] V. Kodur, Properties of concrete at elevated temperatures, *ISRN Civil Engineering*. 2014 (2014).
- [11] A. Lau, M. Anson, Effect of high temperatures on high performance steel fibre reinforced concrete, *Cem. Concr. Res.* 36 (2006) 1698-1707.
- [12] G.A. Khoury, Effect of fire on concrete and concrete structures, *Progress in Structural Engineering and Materials*. 2 (2000) 429-447.
- [13] S.L. Suhaendi, T. Horiguchi, Effect of short fibers on residual permeability and mechanical properties of hybrid fibre reinforced high strength concrete after heat exposition, *Cem. Concr. Res.* 36 (2006) 1672-1678.
- [14] L.T. Phan, High-strength concrete at high temperature-an overview, *Proceedings of 6th International Symposium on Utilization of High Strength/High Performance Concrete*, Leipzig, Germany. (2002) 501-518.
- [15] B. Chen, J. Liu, Residual strength of hybrid-fiber-reinforced high-strength concrete after exposure to high temperatures, *Cem. Concr. Res.* 34 (2004) 1065-1069.
- [16] G.M. Chen, Y.H. He, H. Yang, J.F. Chen, Y.C. Guo, Compressive behavior of steel fiber reinforced recycled aggregate concrete after exposure to elevated temperatures, *Constr. Build. Mater.* 71 (2014) 1-15.
- [17] B. En, 197-1 (2000) *Cement: composition, specifications and conformity criteria for common cements*, British Standards Institution, London. (2000).
- [18] R.H. Haddad, L.G. Shannis, Post-fire behavior of bond between high strength pozzolanic concrete and reinforcing steel, *Constr. Build. Mater.* 18 (2004) 425-435.
- [19] Y. Tai, H. Pan, Y. Kung, Mechanical properties of steel fiber reinforced reactive powder concrete following exposure to high temperature reaching 800 °C, *Nucl. Eng. Des.* 241 (2011) 2416-2424.
- [20] K.K. Sideris, P. Manita, E. Chaniotakis, Performance of thermally damaged fibre reinforced concretes, *Constr. Build. Mater.* 23 (2009) 1232-1239.

Abdallah, S., Fan, M., Cashell, K.A. Pull-out behaviour of straight and hooked-end steel fibres under elevated temperatures. *Cement and Concrete Research*, 2017; 95: 132-140.

<http://www.sciencedirect.com/science/article/pii/S000888461630357X>

[21] K. Wille, A.E. Naaman, Pullout behavior of high-strength steel fibers embedded in ultra-high-performance concrete, *ACI Mater. J.* 109 (2012).

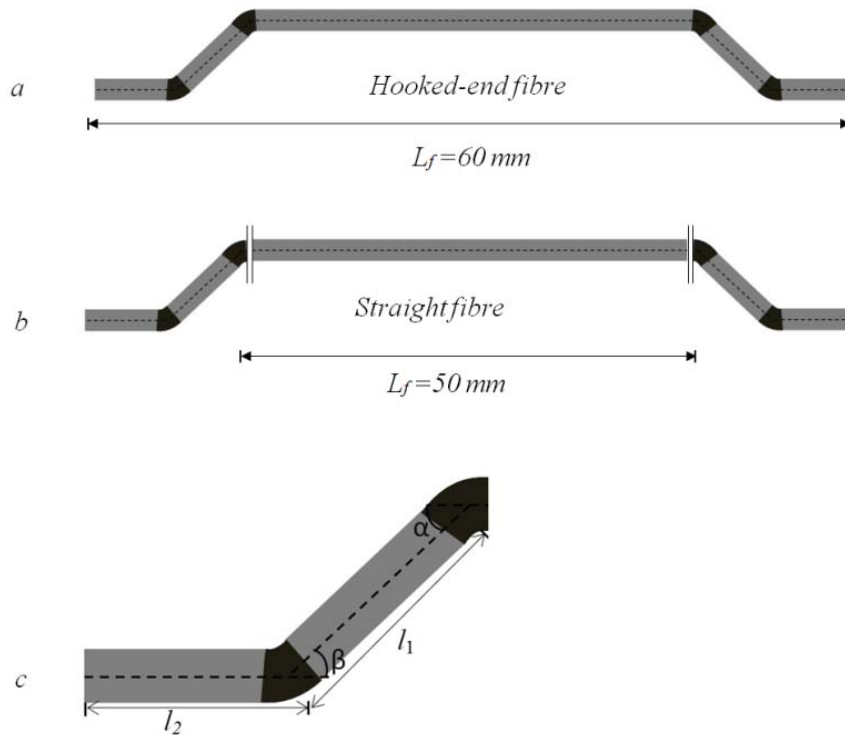


Fig. 1. Geometrical properties of (a) the hooked-end fibres, (b) straight fibres and (c) dimension of hook

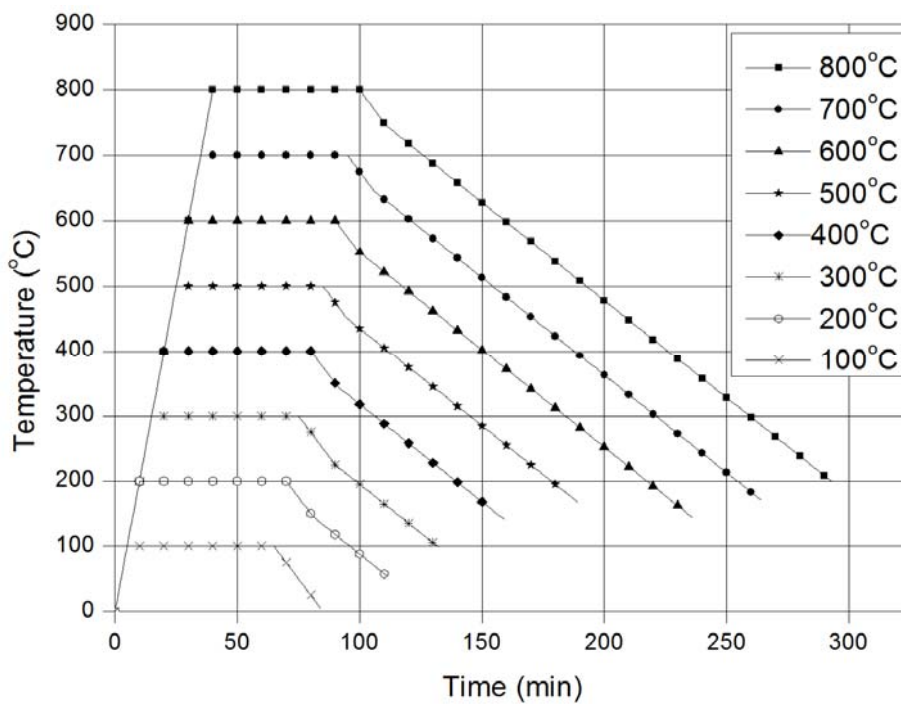


Fig. 2. Time-temperature curves for the elevated temperature tests

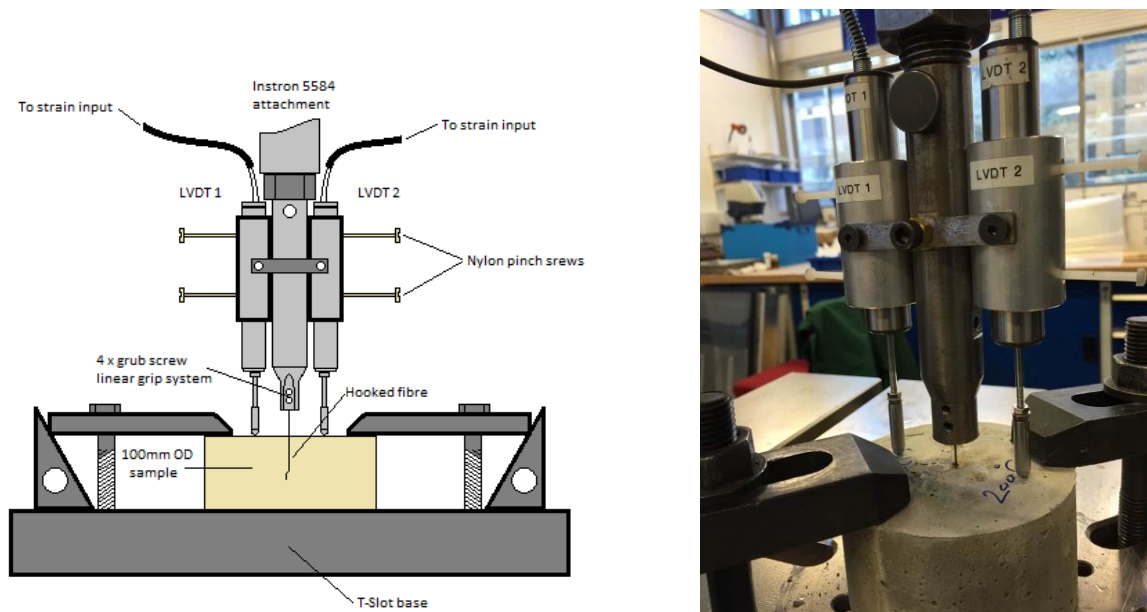


Fig. 3. Pull-out test setup.

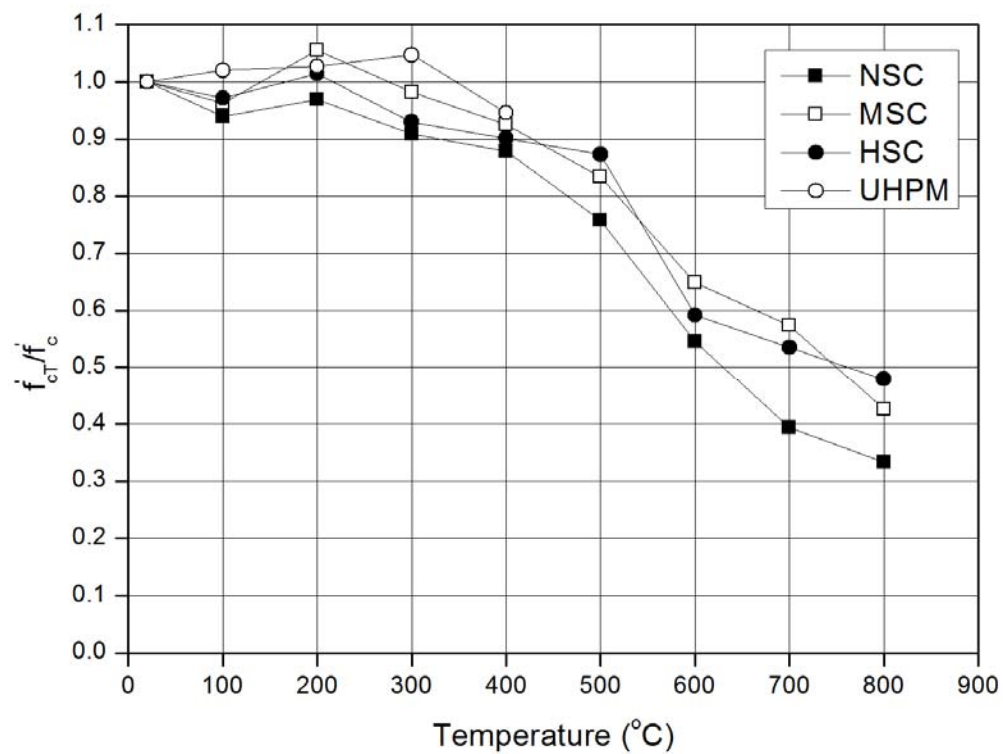


Fig. 4. Effect of temperature on compressive strength.



(a) HSC-800°C

(b) UHPM-500°C

Fig. 5. Failure mode of HSC and UHPM after heating at 800°C and 500°C

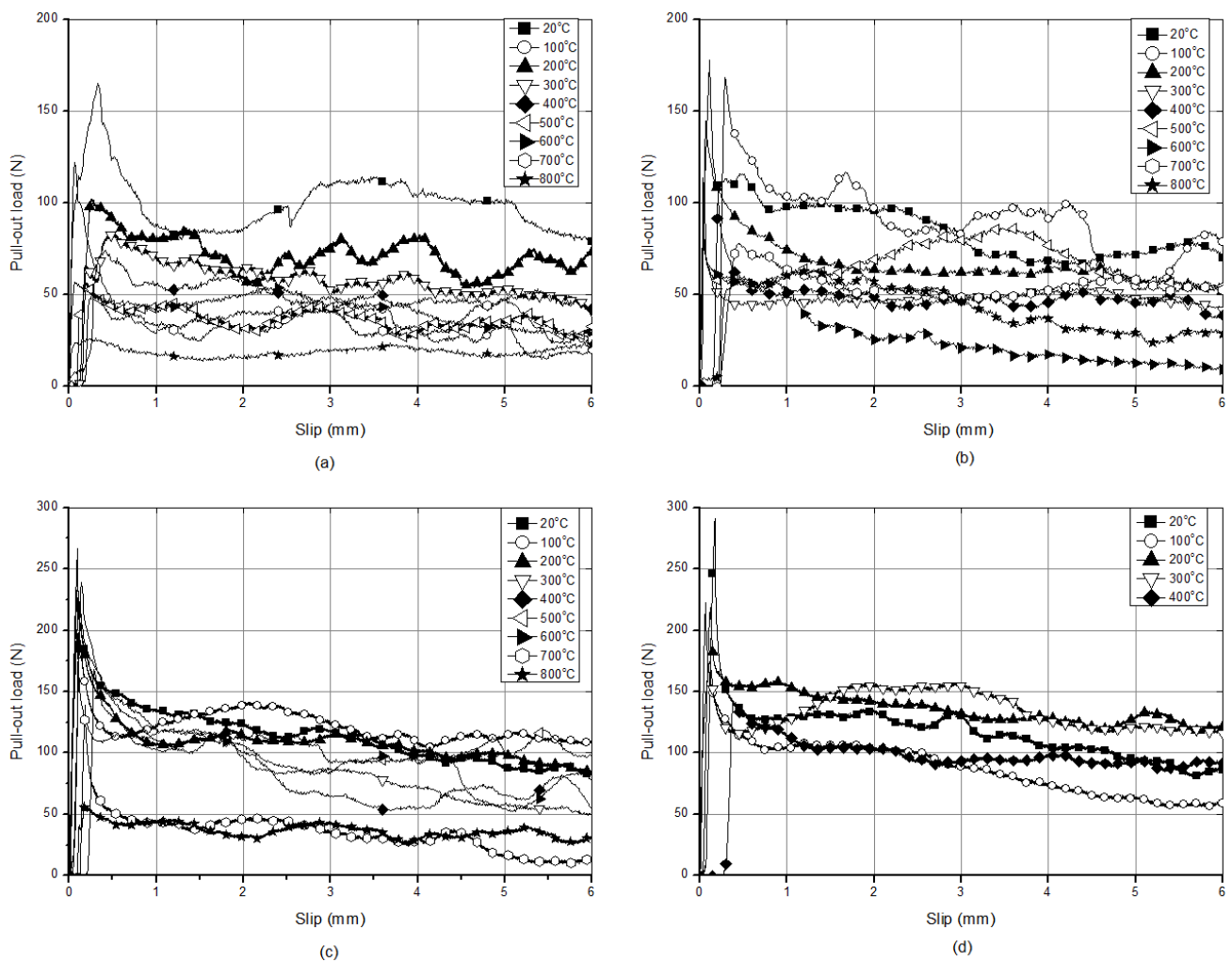


Fig. 6. Pull-out load-slip curves obtained from pull-out test of straight fibre. (a) NSC, (b) MSC, (c) HSC and (d) UHPM.

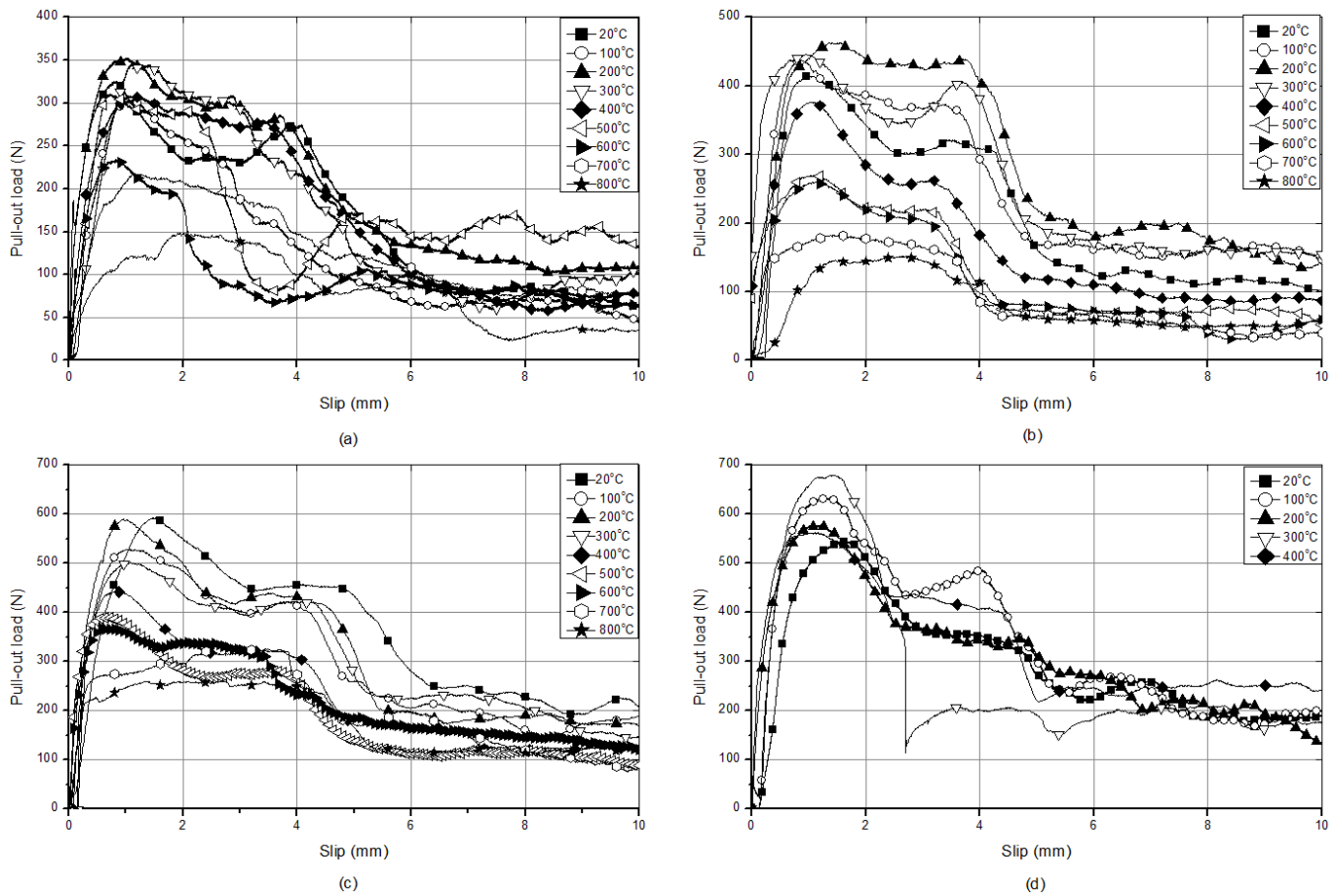


Fig. 7. Pull-out load-slip curves obtained from pull-out tests on hooked end fibres with (a) NSC (b) MSC (c) HSC and (d) UHPM concrete mixes



Fig. 8. Shows the rupture of fibre hook pulled-out from UHPM at 300°C.

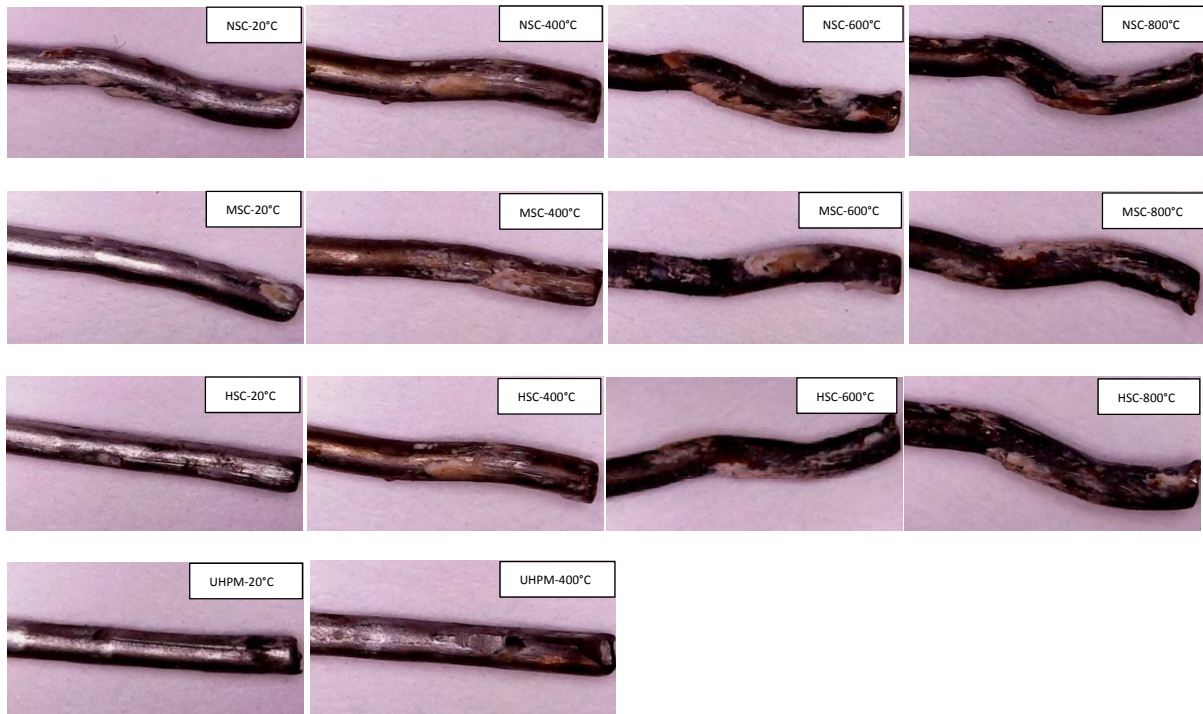


Fig. 9. Deformation and straightening of hook after pull-out test

Table 1 Mix design of mixtures

Matrix type	Cement	Silica fume	Fly ash	Quartz	Aggregate (kg/m ³)			Superplasticizer	Water	W/B
					C.A	F.A				
						C.G.S				
						F.G.S				
					6-8mm	0-4mm	150-600 μm			
NSC	364 ^a	-	-	-	979	812	-	-	200	0.55
MSC	350 ^b	-	107	-	660	1073	-	-	205	0.45
HSC	480 ^b	-	45	-	850	886	-	6	210	0.40
UHPM	710 ^b	230	-	210	-	-	1020	30.7	127	0.11

^a Portland-limestone cement CEM II 32,5R

^b Portland cement CEM III 52.5 N

Table 2 The measured geometric properties of the hooked-end fibres

Fibre type	l_f (mm)	d_f (mm)	f_y (N/mm ²)	l_1 (mm)	l_2 (mm)	α (°)	β (°)
3D 65/60 BG	60	0.90	1150	2.12	2.95	45.7	47.5

Table 3 Test results of mechanical, thermal and pull-out behaviour at elevated temperatures

Material	Property	20°C	100°C	200°C	300°C	400°C	500°C	600°C	700°C	800°C
NSC	f'_c and f'_{cT} (MPa)	33	31	32	30	29	25	18	13	11
	M_{loss} (%)	0	0.16	0.72	1.56	5.95	6.84	7.27	8.89	10.81
	$P_{peak,s}$ (N)	165	122	102	84	74	57	56	52	27
	$S_{peak,s}$ (mm)	0.32	0.06	0.26	0.47	0.41	0.18	0.06	0.29	0.61
	$W_{total,s}$ (Nmm)	2288	1363	1744	721	1040	466	979	527	605
	$P_{peak,h}$ (N)	325	304	352	345	309	310	234	217	148
	$S_{peak,h}$ (mm)	0.79	1.11	0.99	1.13	1.07	0.71	0.81	1.2	2.01
	$W_{total,h}$ (Nmm)	2515	2280	3364	2635	2925	3396	1826	2251	1240
MSC	f'_c and f'_{cT} (MPa)	54	52	57	53	50	45	35	31	23
	M_{loss} (%)	0	0.13	1.92	2.62	6.67	7.65	7.91	8.56	9.85
	$P_{peak,s}$ (N)	177	171	144	113	107	105	104	77	64
	$S_{peak,s}$ (mm)	0.11	0.25	0.77	0.03	0.2	0.06	0.03	0.44	1.36
	$W_{total,s}$ (Nmm)	1066	1236	1504	1089	1162	902	803	757	533
	$P_{peak,h}$ (N)	414	438	463	446	376	269	259	182	151
	$S_{peak,h}$ (mm)	0.96	0.86	1.55	0.96	1.01	1.1	1.13	1.57	2.68
	$W_{total,h}$ (Nmm)	3542	4219	4137	4822	2861	2238	2098	1631	1690
HSC	f'_c and f'_{cT} (MPa)	71	69	72	66	64	62	42	38	34
	M_{loss} (%)	0	0.34	1.69	2.03	3.28	5.81	6.8	7.14	8.25
	$P_{peak,s}$ (N)	266	238	236	227	210	200	168	138	57
	$S_{peak,s}$ (mm)	0.09	0.13	0.09	0.13	0.21	0.07	0.29	0.18	0.19
	$W_{total,s}$ (Nmm)	2263	1932	2271	1871	1815	1558	1442	417	466
	$P_{peak,h}$ (N)	591	589	527	501	442	391	369	335	261
	$S_{peak,h}$ (mm)	1.51	0.96	1.04	1.02	0.86	0.63	0.56	2.73	2.7
	$W_{total,h}$ (Nmm)	6832	4759	5677	5309	4295	3359	3916	3736	3258
UHPM	f'_c and f'_{cT} (MPa)	148	151	152	155	140	-	-	-	-
	M_{loss} (%)	0	0.49	1.14	1.85	2.48	-	-	-	-
	$P_{peak,s}$ (N)	290	222	218	174	141	-	-	-	-
	$S_{peak,s}$ (mm)	0.17	0.06	0.12	0.12	0.39	-	-	-	-
	$W_{total,s}$ (N mm)	2468	1993	1493	1338	702	-	-	-	-
	$P_{peak,h}$ (N)	545	633	577	678	562	-	-	-	-
	$S_{peak,h}$ (mm)	1.61	1.24	1.04	1.45	1.1	-	-	-	-
	$W_{total,h}$ (N mm)	5248	5740	5489	4954	6656	-	-	-	-